

Lifespan extension induced by AMPK and calcineurin is mediated by CRTC-1 and CREB

William Mair^{1,2,3}, Ianessa Morantte^{1,2,3}, Ana P. C. Rodrigues^{1,4}, Gerard Manning^{1,4}, Marc Montminy^{1,3}, Reuben J. Shaw^{1,2,3} & Andrew Dillin^{1,2,3}

Activating AMPK or inactivating calcineurin slows ageing in *Caenorhabditis elegans*^{1,2} and both have been implicated as therapeutic targets for age-related pathology in mammals^{3–5}. However, the direct targets that mediate their effects on longevity remain unclear. In mammals, CREB-regulated transcriptional coactivators (CRTCs)⁶ are a family of cofactors involved in diverse physiological processes including energy homeostasis^{7–9}, cancer¹⁰ and endoplasmic reticulum stress¹¹. Here we show that both AMPK and calcineurin modulate longevity exclusively through post-translational modification of CRTC-1, the sole *C. elegans* CRTC. We demonstrate that CRTC-1 is a direct AMPK target, and interacts with the CREB homologue-1 (CRH-1) transcription factor *in vivo*. The pro-longevity effects of activating AMPK or deactivating calcineurin decrease CRTC-1 and CRH-1 activity and induce transcriptional responses similar to those of CRH-1 null worms. Downregulation of *crtc-1* increases lifespan in a *crh-1*-dependent manner and directly reducing *crh-1* expression increases longevity, substantiating a role for CRTCs and CREB in ageing. Together, these findings indicate a novel role for CRTCs and CREB in determining lifespan downstream of AMPK and calcineurin, and illustrate the molecular mechanisms by which an evolutionarily conserved pathway responds to low energy to increase longevity.

AMPK and calcineurin antagonistically regulate CRTCs in mammals⁸ to modulate energy homeostasis and endoplasmic reticulum (ER) stress^{9,11}. We therefore hypothesized that CRTCs may be critical longevity targets of AMPK and calcineurin, promoting their effects on lifespan through transcriptional regulation. We found a single *C. elegans* CRTC by homology search (Y20F4.2, now re-named CRTC-1) (Fig. 1a and Supplementary Fig. 1). *crtc-1* was expressed throughout the intestine of the worm, as well as in head and tail neurons (Fig. 1b), overlapping the expression pattern of the calcineurin catalytic subunit, *tax-6* (ref. 2) and the AMPK catalytic subunit, *aak-2* (Supplementary Fig. 2a). Strikingly, inhibition of *crtc-1* via RNA interference (RNAi) (Supplementary Fig. 2b) extended wild-type median lifespan by up to 53% (Fig. 1c), comparable to the effects of *tax-6* RNAi or AAK-2 activation (Fig. 1c, d). Given the significant role of CRTC-1 in longevity, we investigated whether AMPK and calcineurin modulate ageing through CRTC-1.

In mammals, activated AMPK blocks the transcriptional function of CRTC2 by restricting it to the cytosol⁹. We therefore tested the effect of starvation and heat stress, two conditions known to activate AMPK in *C. elegans*¹, on CRTC-1 cellular localization. A transgenic strain expressing CRTC-1::RFP revealed that CRTC-1 was present throughout the nucleus and cytosol under basal conditions (Fig. 1e and Supplementary Fig. 2b). Starvation and heat stress both induced CRTC-1::RFP translocation to the cytosol and nuclear exclusion in intestinal cells (Fig. 1f–h and Supplementary Fig. 3), illustrating that environmental stimuli that activate AMPK inactivate CRTC-1.

Next we investigated whether direct activation of AMPK rendered CRTC-1 cytosolic. Mammalian AMPK α catalytic subunits are activated by phosphorylation of threonine 172 in their activation loop. Mutation of this residue to aspartic acid or alanine results in a constitutively active or kinase-dead AMPK, respectively¹². Expression of CRTC-1::RFP with the equivalent activated AAK-2 mutation (amino acids (aa) 1–321, T181D)::GFP, caused nuclear exclusion of CRTC-1 under fed conditions at 20 °C (Fig. 2a). In contrast, coexpression of kinase-dead AAK-2 (aa 1–321, T181A)::GFP and CRTC-1::RFP did not induce nuclear exclusion (Fig. 2a), demonstrating that catalytic activation of AAK-2 by threonine 181 phosphorylation is required for AAK-2-dependent CRTC-1 nuclear exclusion.

Treatment with *tax-6* RNAi caused similar nuclear exclusion of CRTC-1::RFP under fed conditions (Fig. 2b). In addition, tricaine, a class of anaesthetic known to increase calcium flux¹³, induced *tax-6*-dependent nuclear localization of CRTC-1::RFP (Supplementary Fig. 4a). Suggesting CRTC-1 is a direct calcineurin target, CRTC-1::RFP containing site-specific mutations in the calcineurin binding site did not translocate to the nucleus in response to tricaine and was retained in the cytosol (Supplementary Fig. 4b).

Similar to mammalian CRTCs⁸, cytosolic retention of CRTC-1 required 14-3-3 proteins, as simultaneous RNAi knockdown of the two *C. elegans* 14-3-3 proteins *ftt-1* (also known as *par-5*) and *ftt-2* (ref. 14) via RNAi resulted in CRTC-1::RFP accumulation within the nucleus (Fig. 2c) and blocked CRTC-1::RFP cytosolic sequestering after heat stress (Supplementary Fig. 5). In addition, we determined that AMPK directly phosphorylates CRTC-1 at conserved 14-3-3-binding sites. Incubation of CRTC-1 with purified AMPK and AMP in an *in vitro* kinase assay resulted in phosphorylation of CRTC-1, as detected by anti-phospho-Ser 14-3-3 binding motif antibody (Fig. 2d).

Collectively, these data illustrate that in response to pro-longevity perturbations to AMPK and calcineurin, CRTC-1 becomes phosphorylated, cytosolically sequestered and inactivated.

To determine if the lifespan effects of AMPK and calcineurin are due to the inactivation of CRTC-1, we first examined if *crtc-1* RNAi-mediated longevity was epistatic to *tax-6*. Although *crtc-1* RNAi increased the lifespan of wild-type worms, it had no additive effect on the extended lifespan of *tax-6* mutants (Fig. 3a), in which CRTC-1 is already rendered cytosolic and inactive (Supplementary Fig. 4a), suggesting that these lifespan mediators function in a linear pathway.

To examine if CRTC-1 was a direct longevity target of AMPK and calcineurin, we inhibited phosphorylation of CRTC-1 at two conserved AMPK/calcineurin sites, S76 and S179, both of which reside within 14-3-3-binding motifs (Supplementary Fig. 1). Previous studies show that 14-3-3 proteins commonly bind tandem phosphorylated sites within a protein, resulting in significantly increased affinity over solitary sites due to cooperative binding^{15,16}. Compound mutation of serines 76 and 179 to alanines in CRTC-1 rendered it constitutively

¹The Salk Institute for Biological Studies, La Jolla, California 92037, USA. ²Howard Hughes Medical Institute, The Salk Institute for Biological Studies, La Jolla, California 92037, USA. ³The Glenn Foundation for Medical Research, The Salk Institute for Biological Studies, La Jolla, California 92037, USA. ⁴Razavi Newman Center for Bioinformatics, The Salk Institute for Biological Studies, La Jolla, California 92037, USA.

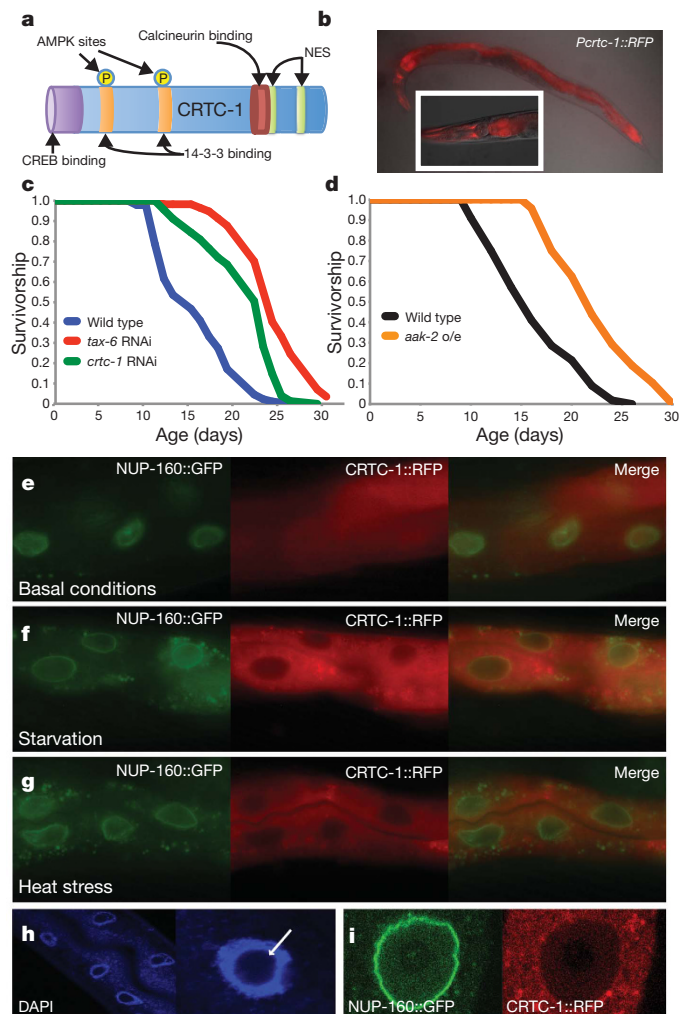


Figure 1 | CRTC-1 regulates longevity. **a**, CRTC-1 is the sole *C. elegans* CRTC family member, with conserved CREB-, calcineurin- and 14-3-3-binding domains and nuclear export signals (NES). Conserved AMPK phosphorylation sites are found at serines 76 and 179. **b**, *Pcrtc-1::RFP* is expressed throughout the intestine of the worm and in neurons in the head (inset) and tail. **c**, RNAi inhibition of *crtc-1* and *tax-6* increases *C. elegans* wild-type median lifespan by 53% and 60% respectively (log rank, $P < 0.0001$ in each case). **d**, Overexpressing *aak-2* (aa 1–321) increases lifespan by 37.5% (log rank, $P < 0.0001$). **e–g**, Coexpression of the NUP-160::GFP nuclear pore complex subunit to mark the nuclear envelope (green), CRTC-1::RFP (red) and merge ($\times 20$ magnification). **e**, Under well-fed conditions CRTC-1::RFP is found throughout intestinal cells. **f, g**, Overnight starvation (**f**) or 33 °C overnight (**g**) induce cytosolic translocation of CRTC-1::RFP. **h**, 4',6-diamidino-2-phenylindole (DAPI) staining of *C. elegans* intestinal nuclei ($\times 20$). White arrow indicates nucleolus. **i**, Confocal image of NUP-160::GFP (green) marking nuclear membrane and CRTC-1::RFP (Red) after 33 °C overnight showing nuclear exclusion of CRTC-1::RFP after heat stress ($\times 100$).

nuclear and refractory to *tax-6* deactivation or *aak-2* activation (Fig. 3b, c and Supplementary Fig. 6).

Notably, although *tax-6* RNAi robustly extended the lifespan of *C. elegans* expressing wild-type CRTC-1::RFP, which translocated to the cytoplasm freely when calcineurin was not present (Fig. 3d), it had no effect on worms expressing constitutively nuclear CRTC-1 (S76A, S179A) (Fig. 3d). Post-translational modification of CRTC-1 is therefore critical for the effects of calcineurin on longevity. This longevity suppression was not due to general sickness as there was no significant difference between the lifespan of wild-type worms and those expressing CRTC-1 (S76A, S179A) (Supplementary Fig. 7a). Knocking down *tax-6* specifically during adulthood again increased wild-type lifespan but had no effect on the CRTC-1 (S76A, S179A) mutant (Supplementary Fig. 7 b–d), indicating that the CRTC-1-dependent effects of *tax-6* on lifespan are not solely acting during development.

We used the CRTC-1 (S76A, S179A) mutant to ask whether the extended lifespan of activated AMPK was also mediated by CRTC-1. Expression of CRTC-1 (S76A, S179A) fully suppressed the lifespan extension seen in AAK-2-overexpressing worms (Fig. 3e). This demonstrates that CRTC-1 is both a critical and direct target of

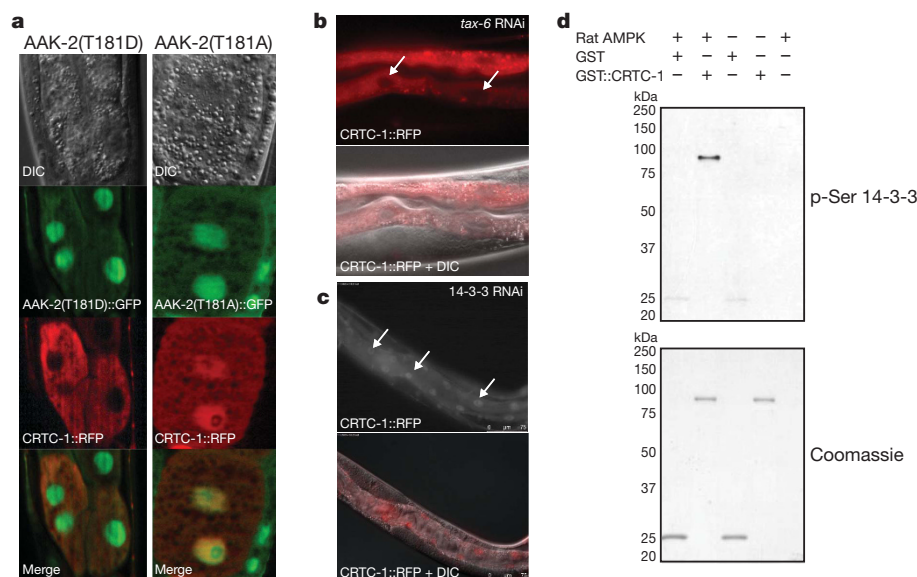


Figure 2 | CRTC-1 is a target of AAK-2 and TAX-6. **a**, CRTC-1::RFP (red) is excluded from the nucleus of intestinal cells when coexpressed with a constitutively active AMPK catalytic subunit AAK-2 (aa 1–321, T181D)::GFP but localized throughout the cell in the presence of kinase-dead AAK-2 (aa 1–321, T181A)::GFP ($\times 63$ magnification). **b**, *tax-6* RNAi results in nuclear exclusion of CRTC-1::RFP (red). White arrows represent intestinal nuclei ($\times 20$). DIC, differential interference contrast microscopy. **c**, Combined RNAi

for the two *C. elegans* 14-3-3 proteins results in nuclear localization of CRTC-1::RFP under basal conditions. White arrows represent intestinal nuclei ($\times 20$). **d**, *In vitro* kinase assay showing that AMPK directly phosphorylates CRTC-1. Purified rat AMPK holoenzyme was incubated with GST or GST::CRTC-1 in the presence of AMP. Phosphorylation was detected with phospho-Ser (p-Ser) 14-3-3 binding motif antibody. Coomassie stained gel shows protein loaded.

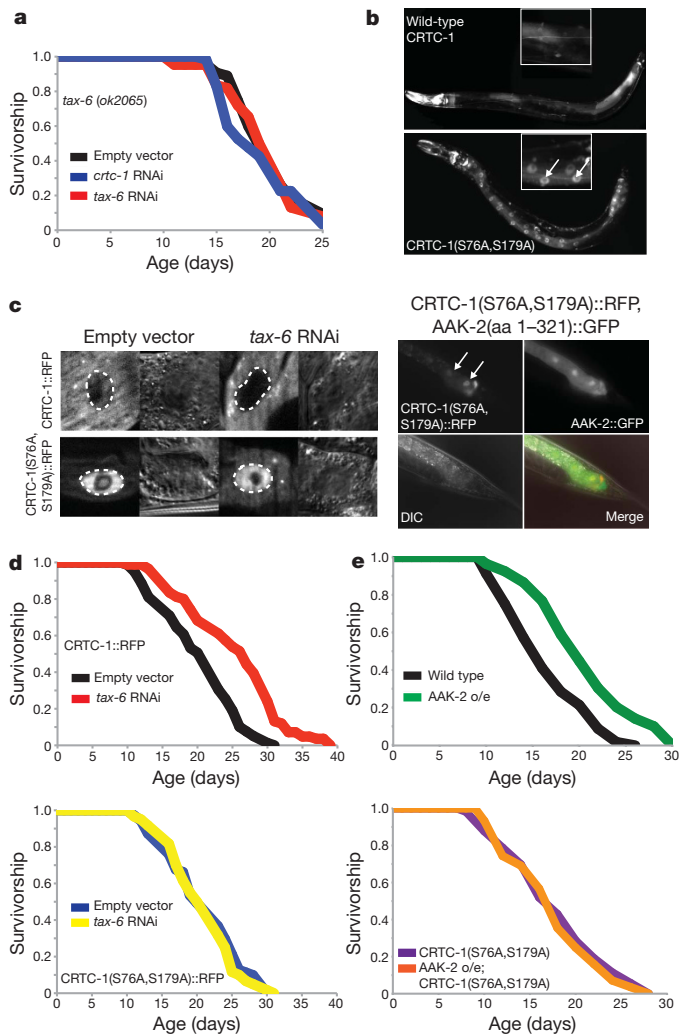


Figure 3 | Calcineurin and AMPK regulate lifespan through phosphorylation of CRTC-1. **a**, RNAi for *crtc-1* or *tax-6* has no effect in a *tax-6* (*ok2065*) mutant background (log rank, $P = 0.28$ and $P = 0.73$, respectively). **b**, Mutations to the conserved AMPK target sites serines 76 and 179 together are sufficient to retain CRTC-1::RFP in the nucleus ($\times 10$). Insets are magnification of intestinal region. **c**, CRTC-1(S76A,S179A) is refractory to both *tax-6* RNAi and AAK-2 overexpressor (*o/e*) in *C. elegans* intestinal cells ($\times 40$). White dashed lines and arrows indicate nuclei. **d**, RNAi of *tax-6* extends the lifespan of *C. elegans* expressing wild-type CRTC-1::RFP (log rank, $P < 0.0001$), but has no effect on the S76A, S179A double mutant (log rank, $P = 0.57$). There is no significant difference between the lifespans of CRTC-1::RFP and CRTC-1(S76A,S179A) fed empty vector (log rank, $P = 0.48$). **e**, AAK-2 (*aa 1–321*) overexpression increases wild-type lifespan (log rank, $P < 0.0001$) but has no effect on worms expressing CRTC-1 (S76A, S179A) (log rank, $P = 0.65$).

aak-2-mediated longevity, and indicates that AMPK and calcineurin function upstream of a shared longevity pathway that signals through CRTC-1.

To understand the downstream effectors of CRTC-1, we examined CRH-1, the single *C. elegans* orthologue of the cyclic AMP response element binding (CREB) transcription factor family¹⁷. Mammalian CREBs (CREB, CREM and ATF1) associate with CRTCs to activate transcription and are involved in diverse processes including memory, immunity, DNA repair, energy homeostasis, fat storage and ER stress^{18,19}. *crh-1* is expressed throughout the worm, in overlapping tissues to *crtc-1* (Supplementary Fig. 8a). Co-immunoprecipitation of Flag::CRTC-1 and HA::CRH-1 demonstrated that these proteins interact *in vivo* (Fig. 4a and Supplementary Fig. 8b). The role of CRTC-1 in CRH-1 transcriptional activation was assessed by the

CREB reporter construct pCRE::GFP, which was significantly repressed by RNAi against *crh-1*, *crtc-1* and *tax-6* (Fig. 4b, c).

If the lifespan extension seen by activating AMPK or deactivating calcineurin functions through CRTC-1 to inactivate CREB, inactivating *crh-1* directly should increase longevity. Indeed, RNAi of *crh-1* increased the lifespan of both wild-type and RNAi-sensitive *rff-3* (*pk1426*) mutants (Fig. 4d and Supplementary Fig. 9). Furthermore, lifespan extension by *crtc-1* RNAi was not seen in *crh-1* (*nn3315*) null mutants (Fig. 4e), indicating that the longevity effects of inactivating *crtc-1* are mediated by *crh-1*.

We examined the effects of AMPK and calcineurin on CREB-regulated genes by comparing whole-genome gene expression of activated *aak-2*, *tax-6* null and *crh-1* null mutant animals to wild-type worms (Supplementary Table 1). Despite the many distinct roles of AMPK and calcineurin, we found that long-lived worms with activated *aak-2* or deactivated *tax-6* had transcriptional profiles significantly similar to *crh-1* null animals (Fig. 4f, g and Supplementary Fig. 10). The directionality of the transcriptional changes induced by activated *aak-2* and inactivated *tax-6* was also remarkably similar to *crh-1* nulls, with the majority of genes (150 or 67.5%) affected by all mutants exhibiting shared patterns of expression (Fig. 4f and Supplementary Fig. 11). Further, differentially expressed genes across all groups were highly enriched for cAMP regulatory elements (CRE) and the presence of a TATA box in their upstream promoter region (Fig. 4h and Supplementary Fig. 12a), two signatures of highly inducible CREB targets. Interestingly, and in contrast to CREB function in mammals, gene expression analysis revealed that CRH-1 may function as a bifunctional transcriptional regulator, as both upregulated and down-regulated genes in *crh-1* null animals were enriched for CREs (Supplementary Fig. 12b).

In mammals, AMPK and CREB are involved in energy homeostasis, particularly in response to starvation. Surprisingly, differentially expressed genes in *aak-2*-overexpressing, *tax-6* null mutant and *crh-1* null mutant animals were not markedly enriched for genes related to metabolism. Rather, there was strong upregulation of genes involved in ER stress, with 55% of known activated in blocked unfolded protein response family members (ABU)²⁰, upregulated by all mutants ($P = 1.7 \times 10^{-8}$, Fisher's exact test; Fig. 4f, Supplementary Fig. 10 and Supplementary Table 2). *abu* genes are induced in response to ER stress when the unfolded protein response pathway (UPR) is blocked and are therefore thought to act in parallel to the UPR to maintain protein homeostasis²⁰. *abu* genes are required for innate immunity²¹ and, notably, are activated by resveratrol and critical for its effects on longevity in *C. elegans*²². Furthermore, overexpression of *abu* family members increases lifespan in the worm²². It will be interesting to determine the potential role of ER stress in lifespan extension via AMPK–calcineurin–CRTC-1 signalling and whether CRTC-1 has a role in resveratrol-mediated lifespan extension.

Our data indicate that CRTC-1 is the critical direct longevity target of both AMPK and calcineurin in *C. elegans* and identify a new role for CRTCs and CREB in modulating longevity. They also represent the first analysis of the transcriptional profiles of long-lived activated AMPK and deactivated calcineurin organisms and suggest the primary longevity-associated role of these perturbations is the modulation of CRTC-1 and CRH-1 transcriptional activity. Notably, both the FOXO transcription factor *daf-16* (ref. 23) and genes involved in autophagy²⁴ have also been implicated in AMPK and calcineurin longevity, respectively. Further work to determine precisely where the AMPK–calcineurin–CRTC-1 pathway converges with FOXO and autophagy will be enlightening. It will also be interesting to determine if CRTC-1 mediates downstream effects of kinases other than AMPK. In mammals, CRTCs are regulated by multiple CAMKL kinase family members^{8,9,25} (Supplementary Table 3), and we saw additive effects of AMPK and related kinases on the localization of CRTC-1, in particular the MAP/microtubule affinity-regulating kinase (MARK) *par-1*, indicating that this kinase may also regulate CRTC-1 *in vivo* (Supplementary Fig. 13c, d). At present,

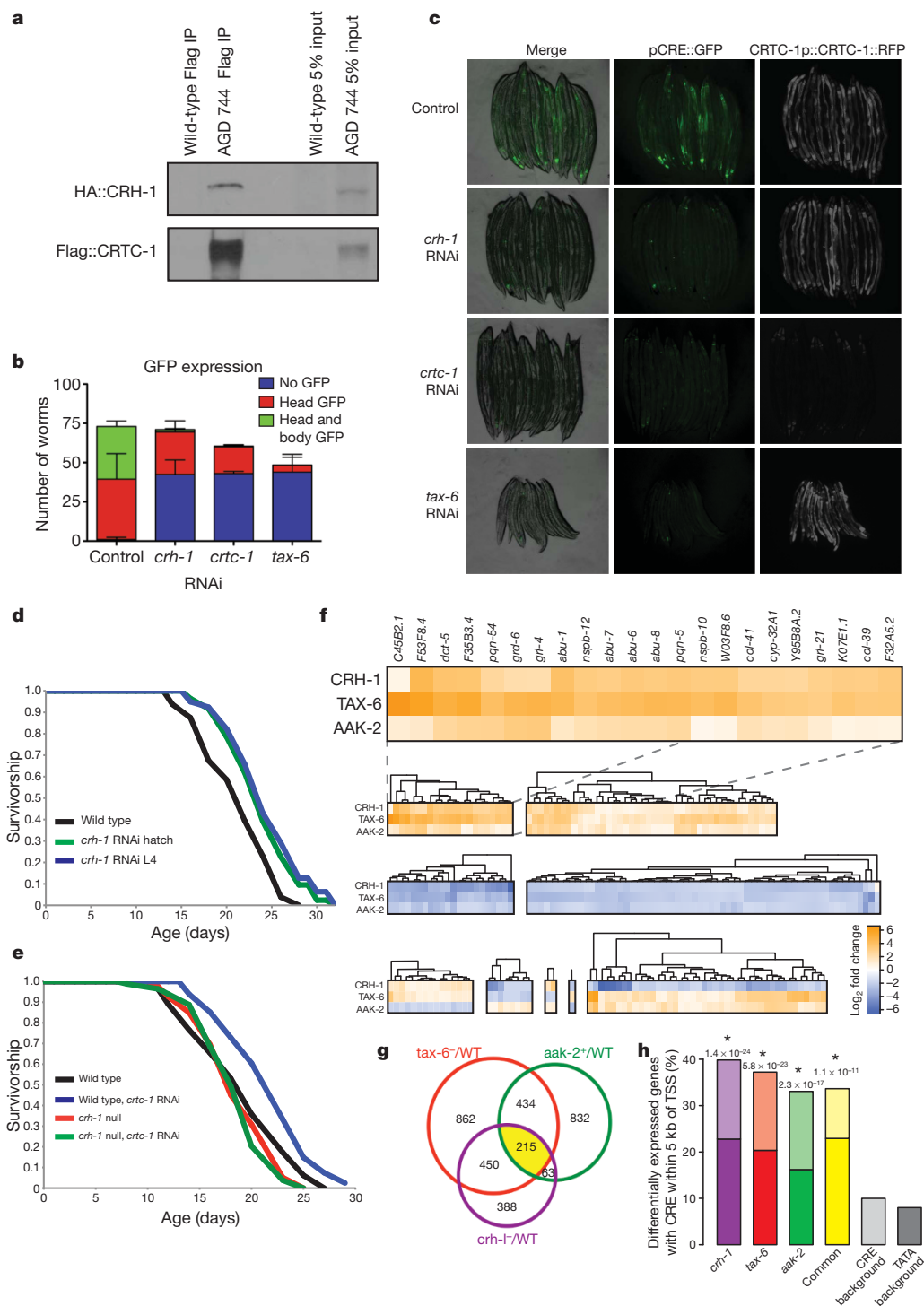


Figure 4 | CREB activity regulates lifespan. **a**, Co-immunoprecipitation using lysate from a *C. elegans* transgenic strain (AGD744) coexpressing 3×Flag::CRTC-1 and HA::CRH-1 showing CRTC-1 and CRH-1 interact *in vivo*. **b**, **c**, CREB transcriptional reporter (pCRE::GFP) is significantly affected by RNAi of *crh-1*, *crtc-1* or *tax-6* (two-way ANOVA, $F = 18.54$, $P < 0.0001$). Error bars represent data \pm s.e.m. Control worms express GFP in head neurons and in some body tissues including muscle, hypodermis and intestine. **d**, RNAi of *crh-1* from larvae or adulthood extends wild-type lifespan (log rank, $P < 0.001$). **e**, RNAi of *crtc-1* extends wild-type lifespan (log rank, $P < 0.001$) but has no effect on *crh-1* (*nn3315*) nulls (log rank, $P = 0.53$). **f**, Heat maps (clustered display of expression relative to wild-type) for genes differentially expressed in *crh-1* (*nn3315*) nulls, *tax-6* (*ok2065*) nulls, and *aak-2*

overexpressors (adjusted P value < 0.05 and fold change larger than twofold). The 22 most upregulated genes in all mutants are expanded (full gene list available in Supplementary Material). **g**, Venn diagram of all differentially expressed genes compared to wild-type in *tax-6* (*ok2065*) nulls, *aak-2* overexpressors and *crh-1* (*nn3315*) nulls. Transcriptional profiles of *aak-2* overexpressors and *tax-6* nulls are more similar to *crh-1* nulls than expected by chance (one-tailed Fisher's exact test, $P = 2.3 \times 10^{-19}$ and $P = 1.1 \times 10^{-225}$, respectively). WT, wild type. **h**, Promoters of differentially expressed genes are significantly enriched for CRE motifs (full bar) and TATA boxes (darker bar) (P values for binomial proportion test compared to CRE background shown above each mutant, asterisks indicate significant P -values). 'Common' denotes genes differentially expressed in all 3 strains. TSS, transcription start site.

however, AMPK is the only CAMKL kinase shown to be a positive regulator of longevity.

Collectively, these data identify CRTC-1 as a central node linking the upstream lifespan modifiers AMPK and calcineurin to CREB activity via a shared signal-transduction pathway, and demonstrate that post-translational modification of CRTC-1 is required for their effects on longevity (Supplementary Fig. 14). Complementing the pro-longevity effects of inhibiting CRTC function in *C. elegans*, reducing components of the CRTC/CREB pathway has recently been shown to confer health benefits to mice^{9,19,26–28}. Given the evolutionary conservation of this pathway from *C. elegans* to mammals²⁹ it will be fascinating to determine the role of CRTCs both as mammalian ageing modulators and as potential drug targets for patients with metabolic disorders and cancer.

METHODS SUMMARY

A detailed description of all experimental methods including *C. elegans* strains (Supplementary Table 4), growth, imaging, lifespan analysis and RNAi application is provided in Methods. None of the RNAi treatments used affected feeding rates (Supplementary Fig. 15). Transgenic strains were generated via microinjection into the gonad of adult hermaphrodites using standard techniques. Integrated transgenic lines were generated using gamma irradiation and outcrossed to wild-type at least four times. All lifespans were conducted at 20 °C with deaths scored and live worms transferred to new plates every 1–2 days, see Supplementary Table 5 for statistical analysis and replicate data. JMP 8/Graphpad Prism 5 and R/Bioconductor software were used for all statistical analyses.

Full Methods and any associated references are available in the online version of the paper at www.nature.com/nature.

Received 29 January; accepted 26 November 2010.

1. Apfeld, J., O'Connor, G., McDonagh, T., DiStefano, P. S. & Curtis, R. The AMP-activated protein kinase AAK-2 links energy levels and insulin-like signals to lifespan in *C. elegans*. *Genes Dev.* **18**, 3004–3009 (2004).
2. Dong, M. Q. *et al.* Quantitative mass spectrometry identifies insulin signaling targets in *C. elegans*. *Science* **317**, 660–663 (2007).
3. Steinberg, G. R. & Kemp, B. E. AMPK in health and disease. *Physiol. Rev.* **89**, 1025–1078 (2009).
4. Supnet, C. & Bezprozvanny, I. Neuronal calcium signaling, mitochondrial dysfunction, and Alzheimer's disease. *J. Alzheimers Dis.* **20** (suppl. 2), 487–498 (2010).
5. Shackelford, D. B. & Shaw, R. J. The LKB1–AMPK pathway: metabolism and growth control in tumour suppression. *Nature Rev. Cancer* **9**, 563–575 (2009).
6. Conkright, M. D. *et al.* TORCs: transducers of regulated CREB activity. *Mol. Cell* **12**, 413–423 (2003).
7. Liu, Y. *et al.* A fasting inducible switch modulates gluconeogenesis via activator/coactivator exchange. *Nature* **456**, 269–273 (2008).
8. Sreaton, R. A. *et al.* The CREB coactivator TORC2 functions as a calcium- and cAMP-sensitive coincidence detector. *Cell* **119**, 61–74 (2004).
9. Koo, S. H. *et al.* The CREB coactivator TORC2 is a key regulator of fasting glucose metabolism. *Nature* **437**, 1109–1111 (2005).
10. Komiya, T. *et al.* Enhanced activity of the CREB co-activator Crtc1 in LKB1 null lung cancer. *Oncogene* **29**, 1672–1680 (2010).
11. Wang, Y., Vera, L., Fischer, W. H. & Montminy, M. The CREB coactivator CRTC2 links hepatic ER stress and fasting gluconeogenesis. *Nature* **460**, 534–537 (2009).
12. Crute, B. E., Seefeld, K., Gamble, J., Kemp, B. E. & Witters, L. A. Functional domains of the $\alpha 1$ catalytic subunit of the AMP-activated protein kinase. *J. Biol. Chem.* **273**, 35347–35354 (1998).
13. Leffler, A. *et al.* The vanilloid receptor TRPV1 is activated and sensitized by local anesthetics in rodent sensory neurons. *J. Clin. Invest.* **118**, 763–776 (2008).
14. Wang, W. & Shakes, D. C. Expression patterns and transcript processing of *ftt-1* and *ftt-2*, two *C. elegans* 14-3-3 homologues. *J. Mol. Biol.* **268**, 619–630 (1997).
15. Kosteletzky, B., Saurin, A. T., Purkiss, A., Parker, P. J. & McDonald, N. Q. Recognition of an intra-chain tandem 14-3-3 binding site within PKC ϵ . *EMBO Rep.* **10**, 983–989 (2009).
16. Johnson, C. *et al.* Bioinformatic and experimental survey of 14-3-3-binding sites. *Biochem. J.* **427**, 69–78 (2010).
17. Kimura, Y. *et al.* A CaMK cascade activates CRE-mediated transcription in neurons of *Caenorhabditis elegans*. *EMBO Rep.* **3**, 962–966 (2002).
18. Mayr, B. & Montminy, M. Transcriptional regulation by the phosphorylation-dependent factor CREB. *Nature Rev. Mol. Cell Biol.* **2**, 599–609 (2001).
19. Xiao, X., Li, B. X., Mitton, B., Ikeda, A. & Sakamoto, K. M. Targeting CREB for cancer therapy: friend or foe. *Curr. Cancer Drug Targets* **10**, 384–391 (2010).
20. Urano, F. *et al.* A survival pathway for *Caenorhabditis elegans* with a blocked unfolded protein response. *J. Cell Biol.* **158**, 639–646 (2002).
21. Haskins, K. A., Russell, J. F., Gaddis, N., Dressman, H. K. & Aballay, A. Unfolded protein response genes regulated by CED-1 are required for *Caenorhabditis elegans* innate immunity. *Dev. Cell* **15**, 87–97 (2008).
22. Viswanathan, M., Kim, S. K., Berdichevsky, A. & Guarente, L. A role for SIR-2.1 regulation of ER stress response genes in determining *C. elegans* life span. *Dev. Cell* **9**, 605–615 (2005).
23. Greer, E. L. *et al.* An AMPK-FOXO pathway mediates longevity induced by a novel method of dietary restriction in *C. elegans*. *Curr. Biol.* **17**, 1646–1656 (2007).
24. Dwivedi, M., Song, H. O. & Ahnn, J. Autophagy genes mediate the effect of calcineurin on life span in *C. elegans*. *Autophagy* **5**, 604–607 (2009).
25. Jansson, D. *et al.* Glucose controls CREB activity in islet cells via regulated phosphorylation of TORC2. *Proc. Natl Acad. Sci. USA* **105**, 10161–10166 (2008).
26. Erion, D. M. *et al.* Prevention of hepatic steatosis and hepatic insulin resistance by knockdown of cAMP response element-binding protein. *Cell Metab.* **10**, 499–506 (2009).
27. Shaw, R. J. *et al.* The kinase LKB1 mediates glucose homeostasis in liver and therapeutic effects of metformin. *Science* **310**, 1642–1646 (2005).
28. Qi, L. *et al.* Adipocyte CREB promotes insulin resistance in obesity. *Cell Metab.* **9**, 277–286 (2009).
29. Lerner, R. G., Depatie, C., Rutter, G. A., Sreaton, R. A. & Balthasar, N. A role for the CREB co-activator CRTC2 in the hypothalamic mechanisms linking glucose sensing with gene regulation. *EMBO Rep.* **10**, 1175–1181 (2009).

Supplementary Information is linked to the online version of the paper at www.nature.com/nature.

Acknowledgements W.M. is funded by the George E. Hewitt Foundation for Medical Research, the American Federation for Aging Research and the Glenn Foundation for Medical Research. R.J.S. is funded by National Institutes of Health (NIH) R01 DK080425 and P01 CA120964. A.P.C.R. and G.M. are funded by NIH R01 HG004164, AG031097 and CA14195. A.D. is supported by NIH R01 DK070696 and AG027463. We thank the *Caenorhabditis* Genetics Center, the National Bioresource Project for the Nematode and Mark Alkema for providing worm strains. We are grateful to M. Raices and M. D'Angelo for critical analysis of the manuscript, DAPI images and the NUP-160::GFP construct. We also thank members of the A.D. laboratory and M. Hansen for comments on the manuscript and discussion and K. Butler for technical assistance in the early stages of this project.

Author Contributions W.M., I.M., M.M., R.J.S. and A.D. designed the experiments. W.M. and I.M. performed the experiments. A.P.C.R. analysed the microarray data and performed the promoter analysis and W.M. analysed and performed statistical analysis on all other data. The manuscript was written by W.M. and edited by I.M., A.P.C.R., G.M., R.J.S. and A.D. All authors discussed the results and commented on the manuscript.

Author Information Data have been deposited at GEO under accession number GSE25513. Reprints and permissions information is available at www.nature.com/reprints. The authors declare no competing financial interests. Readers are welcome to comment on the online version of this article at www.nature.com/nature. Correspondence and requests for materials should be addressed to A.D. (dillin@salk.edu) or R.J.S. (shaw@salk.edu).

METHODS

Lifespan studies. All lifespan experiments were performed on standard 6-cm nematode growth media plates³⁰ supplemented with 100 µg ml⁻¹ carbenicillin at 20 °C. Plates were removed from 4 °C storage 2 days before seeding with 100 µl of *Escherichia coli* HT115 containing either empty vector or RNAi inducing plasmids. RNAi for a particular gene can be readily achieved in the worm by feeding *C. elegans E. coli* (HT115) that express double-stranded RNA of the gene of interest³¹. Bacterial cultures were grown overnight at 37 °C in the presence of both carbenicillin (100 µg ml⁻¹) and tetracycline (10 µg ml⁻¹) before seeding onto NGM plates. Once seeded, bacterial lawns were grown at room temperature (25 °C) for 48 h. RNAi was induced with 100 µl IPTG (100 mM) 2 h before worms were added to plates. To age-synchronize worms, five gravid adults (24 h post larval stage four, L4) were placed on plates with the appropriate control or RNAi bacteria and allowed to lay eggs for 5 h before being removed. These eggs were then cultured to adulthood (72 h post egg lay at 20 °C) before being moved to fresh plates at a density of 10 worms per plate, 10 plates per treatment. Age = 0 was defined as the day adults were moved to 10 worms a plate. Worms were moved to fresh plates every 1–2 days until day 14, after which only those on mould-contaminated plates were transferred. Worms were censored at the first sign of any bacterial contamination. Death was scored by gentle agitation with a worm pick and confirmed with no response after three attempts at both the head and tail. Death was scored every 1–2 days throughout.

RNAi constructs. RNAi *tax-6* and *crh-1* (1) (Supplementary Fig. 9) constructs used were taken from the Vidal RNAi library. The *crtc-1* (1) (Supplementary Fig. 9) RNAi plasmid was made by cloning full-length *crtc-1* cDNA between the two inverted T7 promoters in the pAD12 RNAi plasmid and transformed into HT115 cells. Remaining RNAi constructs used in Supplementary Fig. 9 are in the L4440 plasmid. Primers against cDNA were as follows. CRTC-1 (2): 5'-GG ATCACCGGTTTCAGATGCAT, 3'-AGGTGCACCTTCAGCATTTGT. CRTC-1 (3): 5'-GAGTCCAAGGACATCGAAGTCG, 3'-CTCGAGTGGATGCATTGG AACCATACC. CRH-1 (2): 5'-GAGCTCATGGCCACAATGGCGAG, 3'-CTCG AGCTTATCCGCCGTTTCTA.

DAPI staining. Worms were washed in 1 ml M9 (ref. 30) in a watch glass (1–3 times, until bacteria is removed). M9 was almost completely removed before 100–200 µl DAPI (200 ng ml⁻¹ in ethanol) was added. DAPI treatment was incubated in darkness for 20 min or until the ethanol had evaporated. One millilitre of M9 was then added to rehydrate for 1 h (up to 5 h at room temperature or overnight at 4 °C). One drop (~3 µl) of ProLong mounting medium was placed on a slide before transferring the stained worm. A cover slip was added and sealed with nail polish. Fluorescence was examined at 358 nm.

Heat stress and starvation assays. Effect of heat and starvation on CRTC-1::RFP was measured by placing *C. elegans* expressing *crtc-1::RFP* onto either OP50-seeded NGM plates at 33 °C overnight or into 9-well plates containing M9 media at 20 °C. Controls were *C. elegans* fed OP50 at 20 °C.

Microscopy. All microscopy was performed using 0.1 mg ml⁻¹ tetramisole hydrochloride in M9 as an anaesthetic, which pilot experiments revealed had no effect on CRTC-1 localization. Except for tricaine time-course experiments, worms were in 5 µl anaesthetic mounted on 2% agarose pads on glass slides under glass cover slips. All photographs were taken using a Zeiss Axiovert microscope and AxioCam. Pictures in Figs 2a and 3b used ApoTome optical sectioning. For the tricaine experiments (Supplementary Fig. 4a, b), L4 worms were placed in wells of a 96-well plate in 100 µl of tetramisole/M9 with or without tricaine (2 mg ml⁻¹). Pictures were taken during the time-course through the 96-well plate.

Kinase redundancy assays. Worms were subjected to RNAi for CAMKL kinases from hatch. Twenty-four hours post-L4 worms were then picked into M9 with tricaine (2 mg ml⁻¹) in wells of a 9-well plate. Worms were left on a rotational shaker at 20 °C for 2 h. Using a glass pipette³² worms were then placed onto NG plates seeded with *E. coli* (OP50). When tricaine solution had evaporated (approx 20 min), worms were picked onto fresh OP50 plates, 5 worms per plate. Localization of CRTC-1::RFP was then scored as 'all nuclear' (all intestinal cells showed only punctate nuclear CRTC-1), 'some cells nuclear' (intestinal cells showed mix of punctate nuclear CRTC-1 and cytosolic CRTC-1) and 'cytosolic' (CRTC-1 was dispersed evenly throughout nucleus and cytosol in all intestinal cells). Time = 0 was defined as when worms were moved to fresh OP50 plates.

Transgenic strain construction. Expression constructs were based on pPD95.77 from the Fire laboratory *C. elegans* vector kit. RFP in the manuscript refers to tdTOMATO, which replaced the GFP in pPD95.77. Transgenic strains were generated via microinjection into the gonad of adult hermaphrodites using standard techniques. Integrated transgenic lines were generated using gamma irradiation and out-crossed to wild-type at least four times.

Calcineurin-binding mutant. QuikChange mutagenesis was used to mutate residues within the conserved calcineurin-binding site in CRTC-1. This resulted

in changing the amino acid sequence (aa 423–428) as follows. Wild type: EALDIPKLITITNAEGA; calcineurin-binding mutant: EALDIAKATAANAEGA. **Single-worm PCR for genotyping.** Single-worm lysis buffer (SWLB): 30 mM Tris pH 8.0, 8 mM EDTA, 100 mM NaCl, 0.7% NP-40, 0.7% Tween-20. Proteinase K was added to a final concentration of 100 µg ml⁻¹ just before use. To prepare the DNA template, one worm was added to a PCR tube containing 5 µl SWLB supplemented with Proteinase K and incubated for 60 min at 60 °C. Proteinase K was then heat-inactivated at 95 °C for 15 min before the reaction was cooled to 4 °C. To setup the PCR reaction, 5 µl of the worm lysate was used as template.

Expression of *C. elegans* proteins in 293T cells. Full-length *C. elegans crtc-1* and *crh-1* cDNA was cloned using gateway recombination into mammalian expression plasmid pcDNA3 containing in-frame 5' Flag or HA tag respectively. 293T cells were transfected using lipofectamine 2000 (Invitrogen) following manufacturer's guidelines. Primer information is available on request.

293T cells immunoprecipitation. 293T cells were washed 1× with PBS and resuspended in 500 µl PLB supplemented with protease inhibitor cocktail (Roche). Cells were incubated for 10 min at 4 °C then sonicated to disrupt nuclei. Lysate was centrifuged at 10,000g for 30 min at 4 °C then precleared with Protein A/G PLUS-Agarose (Santa Cruz). Cleared lysate was incubated with anti-Flag M2 affinity gel (Sigma) overnight at 4 °C. For control anti-Flag M2 affinity gel was blocked with 50 µg Flag peptide for 1 h at 4 °C then lysate was added and incubation continued overnight at 4 °C. Immune complexes were collected by centrifugation and washed extensively. Complexes were eluted with Flag peptide then resolved by SDS-PAGE and transferred to nitrocellulose membrane. Western blot analysis was performed with anti-Flag M2-Peroxidase (Sigma) and anti-HA-Peroxidase (Roche).

***C. elegans* immunoprecipitation.** Approximately 25,000 N2 and AGD 744 animals were treated with 2 mg ml⁻¹ Tricaine for 2 hours, flash-frozen, then ground to fine powder using a mortar and pestle on dry ice. Powder was collected in 400 µl cell lysis buffer (Cell Signaling) supplemented with protease inhibitor cocktail (Roche) and sonicated to disrupt nuclei. Lysate was centrifuged at 16,000g for 30 min at 4 °C then precleared with Protein A/G PLUS-Agarose (Santa Cruz). Cleared lysate was incubated with EZview Red anti-Flag M2 affinity gel (Sigma) for 2 h at 4 °C. Immune complexes were collected by centrifugation and washed extensively. Complexes were eluted with 3× Flag peptide then resolved by SDS-PAGE and transferred to nitrocellulose membrane. Western blot analysis was performed with anti-Flag M2-Peroxidase (Sigma) and anti-HA (Abcam).

In vitro kinase assay. Recombinant GST::CRTC-1 and GST proteins (2 µg) were incubated with 100 mU purified AMPK (Millipore) in kinase reaction buffer (2.5 mM Tris, pH 7.5, 5 mM β-glycerophosphate, 2 mM DTT, 0.1 mM Na₃VO₄, 10 mM MgCl₂, 150 µM AMP, 125 µM ATP) for 30 min at 30 °C. Samples were resolved by SDS-PAGE then transferred to nitrocellulose membrane. Phosphorylation was determined by immunoblotting with phospho-Ser 14-3-3-binding motif antibody (Cell Signaling).

Microarray procedure. Egg preparations were made using standard bleaching techniques and larval stage one (L1) worms were synchronized by hatching eggs overnight in M9 buffer. Seven hundred and fifty L1 larvae were seeded per 10 cm NG plate seeded with OP50. Worms were harvested for RNA extraction when they reached L4 larval stage by snap-freezing in liquid nitrogen in TRIzol. All L1 larvae were seeded at the same time and samples frozen at different times to account for variation in development time between groups. Three thousand worms were used for each sample and three biological replicates done for each experimental group: N2, AGD383, RB1667 and *crh-1* (*nn3315*). Biological samples were prepared on separate days, RNA preparations were carried out at the same time (12 h before array) using TRIzol/chloroform extraction and then run through an RNeasy cleanup column. Arrays were done on Affymetrix *C. elegans* Genome Array from the same batch.

Microarray data analysis. Raw expression data files were obtained for three replicates each of L4 *crh-1* (*nn3315*), *tax-6* (*ok2065*) and *aak-2* (*aa1-321*) mutants and three N2 control replicates with the Affymetrix *C. elegans* Genome Array. All microarray analysis was performed with Bioconductor³³. Standard data quality validation as suggested by Affymetrix³⁴ was carried out with the 'simpleaffy' package, followed by 'affyPLM', which identified no problematic chips. The raw data were preprocessed according to the GC-RMA method³⁵ (implemented in 'gcrma'), which performs probe-sequence-based background adjustment, quantile normalization, and utilizes a robust multi-chip average to summarize information into single expression measurements for each probeset (Supplementary Table 1). Before statistical testing, the data were submitted to a non-specific filter (via the package 'genefilter') that removed probesets with an expression interquartile range smaller than 0.5. To identify genes that were significantly differentially expressed between each mutant and the control, linear modelling and empirical Bayes analysis was performed using the 'limma' package³⁶. Limma computes an empirical Bayes adjustment for the *t*-test (moderated *t*-statistic), which is more robust than

the standard two-sample *t*-test comparisons. To correct for multiple testing, Benjamin and Hochberg's method to control for false discovery rate was used³⁷. Genes with an adjusted *P* value of 0.05 or smaller and a fold-change in expression larger than twofold were considered differentially expressed (Supplementary Table 2).

cAMP response element (CRE) identification. We gathered intergenic upstream sequences (up to 5 kb, from WS198) for differentially expressed genes and used MATCH³⁸ to search against the TRANSFAC³⁹ CRE matrix (M00039), an experimentally derived matrix based on 29 human CREB1-binding sequences⁴⁰. In the MATCH search we used the 'minFP' score cutoff, which aims to minimize false positives. In addition, we estimated the number of such sites that can be found by chance (background) by using the same procedure to search the upstream sequences of ten similarly sized samples of *C. elegans* genes that were not affected by any of the mutants. We used the same procedure to search against the TRANSFAC TATA matrix (M00252)⁴¹.

30. Hope, I. A. *C. elegans: A Practical Approach* (ed. Hames, B. D.) (Oxford Univ. Press, 1999).
31. Fire, A. *et al.* Potent and specific genetic interference by double-stranded RNA in *Caenorhabditis elegans*. *Nature* **391**, 806–811 (1998).
32. Mair, W. A simple yet effective method to manipulate *C. elegans* in liquid. *Worm Breed. Gaz.* **18**, 33 (2009).
33. Gentleman, R. C. *et al.* Bioconductor: open software development for computational biology and bioinformatics. *Genome Biol.* **5**, R80 (2004).
34. Affymetrix. *GeneChip Expression Analysis* (http://www.coriell.org/images/pdf/expression_manual.pdf) (Affymetrix, 2004).
35. Wu, Z., Irizarry, R. A., Gentleman, R., Martinez-Murillo, F. & Spencer, F. A model-based background adjustment for oligonucleotide expression arrays. *J. Am. Stat. Assoc.* **99**, 909–917 (2004).
36. Smyth, G. K. Linear models and empirical Bayes methods for assessing differential expression in microarray experiments. *Stat. Appl. Gen. Mol. Biol.* **3**, article 3 (2004).
37. Benjamini, Y. & Hochberg, Y. Controlling the false discovery rate: a practical and powerful approach to multiple testing. *J. R. Stat. Soc. B* **57**, 289–300 (1995).
38. Kel, A. E. *et al.* MATCH: a tool for searching transcription factor binding sites in DNA sequences. *Nucleic Acids Res.* **31**, 3576–3579 (2003).
39. Matys, V. *et al.* TRANSFAC and its module TRANSCOMP: transcriptional gene regulation in eukaryotes. *Nucleic Acids Res.* **34**, D108–D110 (2006).
40. Benbrook, D. M. & Jones, N. C. Different binding specificities and transactivation of variant CRE's by CREB complexes. *Nucleic Acids Res.* **22**, 1463–1469 (1994).
41. Bucher, P. Weight matrix descriptions of four eukaryotic RNA polymerase II promoter elements derived from 502 unrelated promoter sequences. *J. Mol. Biol.* **212**, 563–578 (1990).